Published in final edited form as:
Biomaterials. 2012 October ; 33(28): 6709–6720. doi:10.1016/j.biomaterials.2012.06.017.

The effect of controlled release of PDGF-BB from heparin-conjugated electrospun PCL/gelatin scaffolds on cellular bioactivity and infiltration

Jongman Lee, **James J. Yoo**, **Anthony Atala**, and **Sang Jin Lee***
Wake Forest Institute for Regenerative Medicine, Wake Forest School of Medicine, Medical Center Boulevard, Winston-Salem, NC 27157, USA

Abstract

Heparin-conjugated electrospun poly(ε-caprolactone) (PCL)/gelatin scaffolds were developed to provide controlled release of platelet-derived growth factor-BB (PDGF-BB) and allow prolonged bioactivity of this molecule. A mixture of PCL and gelatin was electrospun into three different morphologies. Next, heparin molecules were conjugated to the reactive surface of the scaffolds. This heparin-conjugated scaffold allowed the immobilization of PDGF-BB via electrostatic interaction. *In vitro* PDGF-BB release profiles indicated that passive physical adsorption of PDGF-BB to non-heparinized scaffolds resulted in an initial burst release of PDGF-BB within 5 days, which then leveled off. However, electrostatic interaction between PDGF-BB and the heparin-conjugated scaffolds gave rise to a sustained release of PDGF-BB over the course of 20 days without an initial burst. Moreover, PDGF-BB that was strongly bound to the heparin-conjugated scaffolds enhanced smooth muscle cell (SMC) proliferation. In addition, scaffolds composed of 3.0 μm diameter fibers that were immobilized with PDGF-BB accelerated SMC infiltration into the scaffold when compared to scaffolds composed of smaller diameter fibers or scaffolds that did not release PDGF-BB. We concluded that the combination of the large pore structure in the scaffolds and the heparin-mediated delivery of PDGF-BB provided the most effective cellular interactions through synergistic physical and chemical cues.

Keywords

Scaffold; Heparin; Bioactivity; Protein delivery; Cellular infiltration; Vascular tissue engineering

1. Introduction

Electrospinning is a versatile technique that has been utilized to produce tissue engineering scaffolds and drug/protein delivery vehicles. Electrospinning technology, which uses high-voltage electrostatic fields to generate fibrous structures, provides a biomimetic cellular environment which resembles the extracellular matrix (ECM) of native tissues by permitting fabrication of nano- to micro-scale fibers which are able to interact with cells [1–4]. Moreover, the inherently high surface area to volume ratio and high pore interconnectivity associated with electrospun fibers allow for high drug loading efficiency and the ability to overcome mass transfer limitations associated with other polymeric delivery systems. These electrospun materials have been tested in experiments designed to facilitate drug diffusion and improve the solubility of various bioactive molecules [1,5,6].

*Corresponding author. Tel.: +1 336 713 7288; fax: +1 336 713 7290. sjlee@wakehealth.edu (S.J. Lee).

In order to deliver bioactive molecules via electrospun fibers, emulsion and coaxial electrospinning have been recently developed to create core-shell structures from electrospun fibers. Emulsion electrospinning utilizes emulsions made of an oil phase, which contains the polymer solutions in an organic solvent, and a water phase, which contains the drug or protein to be incorporated into the electrospun fibers [7]. On the other hand, coaxial electrospinning utilizes a setup in which an aqueous solution, containing dissolved drugs or proteins, is co-electrospun within a polymer solution, which forms the outer core-shell structure [8]. However, exposure to high voltage and organic solvents may denature incorporated bioactive molecules and destroy their biological activity during the electrospinning process [9]. Moreover, due to the high solubility of most bioactive molecules, they are often released in a rapid initial burst and may have short diffusion pathways [10].

To overcome these limitations, we previously developed a heparin-conjugated electrospun PCL/gelatin scaffold that can release lysozyme (isoelectric point = pH 10.7) as a model protein in a controlled manner [11]. Because heparin is a highly sulfated glycosaminoglycan which possesses strong binding affinity for a variety of growth factors, including basic fibroblast growth factor (bFGF), transforming growth factor-β (TGF-β), vascular endothelial growth factor (VEGF), and platelet-derived growth factor-BB (PDGF-BB) [12–14], it is an excellent choice for this purpose. It has been demonstrated that a sustained release of growth factors over a long period was effectively achieved using heparin conjugation, with the secondary benefit of protected bioactivity. The interaction of growth factors with heparin is considered to be essential for storage, release, and protection from heat, pH, and enzymatic degradation [12].

Additionally, the small-sized pores within many electrospun fibrous scaffolds limit adequate cellular infiltration. To improve the pore structure of these scaffolds, several approaches have been proposed to generate larger-sized pores. These include the use of the salt leaching technique [15] and co-electrospinning with water-soluble polymers which serve as sacrificial fibers [16]. However, these approaches may decrease the mechanical properties and dimensional stability required to maintain structural integrity of a scaffold under physiological conditions. However, we previously demonstrated that these pores can be expanded by increasing the fiber diameter within electrospun scaffolds, and this serves to better accommodate cellular infiltration [2].

In this study, we fabricated heparin-conjugated electrospun PCL/gelatin fibrous scaffolds with different fiber diameters and morphologies, and then immobilized PDGF-BB on the scaffolds to enhance the cellular interactions between vascular smooth muscle cells (SMCs) and the scaffold material. PDGF-BB has been shown to act as a chemotactic agent that causes SMCs to proliferate and migrate [17]. We examined the *in vitro* release kinetics and bioactivity of PDGF-BB from the heparin-conjugated scaffolds. Finally, we also determined whether PDGF-BB conjugation increased SMC infiltration into the electrospun scaffolds over a 4-week period *in vitro*.

2. Materials and methods

2.1. Electrospun PCL/gelatin fibrous scaffolds

The basic set-up used for electrospinning consisted of a syringe pump (Medex Inc., Lauderdale, FL, USA), a high-voltage generator (Spellman High Voltage, Hauppauge, NY, USA), and a collecting mandrel (41.1 mm in diameter). A positive charge of 12 kV was applied to the tip of the syringe needle, and a gap distance between the syringe needle and the grounded collector was 15 cm.

A polymer blend of poly(ε-caprolactone) (PCL, Intrinsic viscosity = 1.77 dL/g, Lactel Absorbable Polymers, Birmingham, AL, USA) and gelatin (derived from porcine skin, Sigma Chemical Co., St. Louis, MO, USA) was electrospun as follows. A 1:1 weight ratio of PCL and gelatin was dissolved in 1,1,1,3,3,3-hexafluoro-2-propanol (HFIP) to make both 10% (w/v) and 15% (w/v) solutions. Each of the solutions (10% and 15%) was electrospun individually to fabricate two different fiber morphologies (small and large diameters). In order to obtain a combination of small and large diameters, both blend solutions (10% and 15%) were co-electrospun using two separate syringe pumps which were placed facing each other while a collecting mandrel was positioned between them. The PCL/gelatin blend solution was ejected via a 20 gauge blunt needle at a constant flow rate of 2–5 ml/h. Electrospun fibers were collected on the cylindrical mandrel, which rotated at a rate of about 1000 rpm and was kept in a vacuum desiccator between uses. All chemical reagents were obtained from Sigma Chemical Co. unless stated otherwise.

Crosslinking of electrospun PCL/gelatin scaffolds was performed in an ethanol solution containing 25 mM 1-ethyl-3-(3-dimethylaminopropyl)carbodiimide (EDC, Thermo Scientific, Waltham, MA, USA) and 10 mM N-hydroxysuccinimide (NHS) for 15 min. For the analysis of fiber morphology, the electrospun PCL/gelatin scaffolds were sputter-coated with gold (Hummer™ 6.2, Anatech Ltd, Denver, NC, USA) and observed using scanning electron microscopy (SEM, S-2260N, Hitachi Co. Ltd, Japan). The diameter distribution of the electrospun fibers created from each electro-spinning condition was determined by selecting twenty fibers at random from three images, measuring the diameter, and expressing the result as a mean and standard deviation (n =20) with the aid of Image J software (NIH, Bethesda, MD, USA).

2.2. Preparation of heparin-conjugated electrospun scaffolds and PDGF-BB immobilization

A brief overview of heparin conjugation and subsequent PDGF-BB immobilization on electrospun PCL/gelatin scaffolds is illustrated in Fig. 1A. In the first step of the process, the reactive amine groups ($-NH_2$) on the PCL/gelatin scaffolds were conjugated with the carboxyl groups (−COOH) on the heparin molecules such that an amide bond (covalent bond formation) was created between them. This process allowed the negatively charged sulfonic groups ($-SO_3$) in the heparin molecules to subsequently trap added PDGF-BB via electrostatic interaction.

Heparin conjugation of the electrospun PCL/gelatin scaffolds (1×1 cm^2) with different fiber morphologies was performed as follows. According to our previous studies [11] on the relationship between residual amine groups and crosslinking period, we determined that a 15 min crosslinking time for the electrospun PCL/gelatin scaffolds used in this study was optimal. The crosslinked PCL/gelatin scaffolds were then equilibrated with 0.05 M of 2-morpholinoethane sulfonic acid buffer (MES, pH 5.6) for 30 min. Heparin sodium salt was dissolved at a concentration of 1 mg/ml in 0.05 M MES buffer containing 25 mM EDC/10 mM NHS to ensure that the carboxyl groups of heparin were activated. One ml of this heparin solution was added to each sample and the samples were incubated at room temperature for 4 h with gentle shaking. During this step, the chemical conjugation between the carboxyl groups of heparin and the amine groups of gelatin occurred. After 4 h, the heparin-conjugated PCL/gelatin scaffolds were washed with 0.1 M Na2HPO4 and distilled water (three times each). The amount of conjugated heparin was quantified using a Toluidine Blue assay. In brief, the heparin-conjugated electrospun PCL/gelatin scaffolds were incubated with 1 ml of Toluidine Blue solution (0.4 mg/ml Toluidine Blue O, 2 mg/ml $NaCl_2$, and 0.1 M HCl) for 2 h at room temperature with gentle agitation to create dye–heparin complexes. Samples were rinsed with distilled water twice for 5 min, and the residual Toluidine Blue that was bound to the heparin was solubilized with a mixture of 0.1

M NaOH and ethanol (1:4). The absorbance of the resulting solution was measured at 530 nm using a spectrophotometer (SpectraMax M5, Molecular Devices, Sunnyvale, CA, USA).

Some scaffolds were then reacted with PDGF-BB (24.3 kDa, isoelectric point: 9.8, Peprotech, Rocky Hill, NJ, USA) at a concentration of 100 ng per sample (0.1% NaN_3 in PBS) for 7–8 h at 4 °C. Shortly after the PDGF-BB immobilization process, the samples were washed with PBS (three times) and stored at 4 °C until needed.

2.3. In vitro release kinetics of PDGF-BB from heparin-conjugated scaffolds

PDGF-BB is known to bind to heparin molecules mainly via electrostatic interaction [18]. Thus, we anticipated that PDGF-BB would be able to interact with the heparin moieties on the electrospun PCL/gelatin scaffolds. The PDGF-BB release test was designed to determine the influence of heparin conjugation and fiber morphology (diameter) on the release profiles of PDGF-BB. To fabricate a control group, electrospun scaffolds of three different fiber morphologies (1.0 μm, co-electrospun, and 3.0 μm fibers) that had not been conjugated with heparin were passively adsorbed with the same amount of PDGF-BB (100 ng) for 7–8 hat4°Cand these control scaffolds were compared to the heparin-conjugated scaffolds immobilized with PDGF-BB.

To analyze the release kinetics of PDGF-BB from PCL/gelatin scaffolds, the PDGF-BB loaded electrospun scaffolds (1×1 cm^2) with or without heparin were placed in 5 ml tubes, and 2 ml of release media (0.1% bovine serum albumin and 0.1% NaN3 in PBS) was added to each tube. These samples were then incubated at 37 °C with gentle shaking at 150 rpm for up to 20 days. At predetermined time points, all of the media (2 ml) in each tube was replaced with fresh media to maintain infinite sink conditions at each time point. The cumulative amount of PDGF-BB in the release media from each sample was analyzed using a human PDGF-BB ELISA Development Kit (Peprotech, Rocky Hill, NJ, USA) according to the manufacturer's instructions. The amount of PDGF-BB released from each scaffold was normalized to the dry weight of each sample ($n = 3$).

2.4. Determination of biological activity of PDGF-BB released from scaffolds

The bioactivity of PDGF-BB that was released from as well as bound to the electrospun PCL/gelatin scaffolds (1×1 cm^2) was evaluated using a human smooth muscle cell (hSMC) culture system (Lonza, Basel, Switzerland), as these cells respond to PDGF-BB by increasing proliferation in culture. Human SMCs were maintained in smooth muscle cell basal medium (SmBM, Lonza) supplemented with fetal bovine serum (FBS), human recombinant FGF-2, human recombinant epidermal growth factor (EGF), human recombinant insulin, and gentamicin sulfate/amphotericin-B under standard culture conditions at 37 °C, 5% CO2. When the cells reached 70–80% confluence, they were trypsinized and collected by centrifugation. The scaffolds were sterilized by immersion in 70% ethanol for 2–3 h and were then washed with PBS repeatedly to completely remove all traces of the ethanol.

To measure the bioactivity of PDGF-BB released from the scaffolds, hSMCs were seeded on 24-well tissue culture plates at a density of 1×10^4 cells/well, and 1 ml of the supplemented SmBM media was added to each well. After incubating the cells overnight to allow them to adhere to the tissue culture plates, the cells were washed with PBS twice. Transwell® membrane inserts Corning Inc., Corning, NY, USA), which had been embedded with the sterilized scaffolds, were then placed into the 24-well tissue culture plates, and 1 ml of basal medium containing 1% FBS (serum-deficient medium) was added to each well. This serum-deficient medium was replaced every other day throughout the experiment. On days 3 and 7 after addition of the Trans-well® inserts, the metabolic activity of the cells was

measured using a colorimetric MTS assay (CellTiter 96® AQeous One solution Cell Proliferation Assay, Promega, Fitchburg, WI, USA) according to the manufacturer's instructions. The absorbance at 490 nm was measured using a spectrophotometer (SpectraMax M5, Molecular Devices). The absorbance value was related to the amount of formazan production by the cells in each well, and this was directly proportional to the number of living cells growing on the culture plates ($n = 3$).

In order to measure the bioactivity of PDGF-BB that was bound to the fibers within the scaffolds, 2×10^4 cells were seeded on each scaffold in a culture dish, and these cultures were maintained statically for 4–5 h to improve cell adhesion. After this period, the samples were incubated overnight in 1 ml of the supplemented medium. The following day, the cell-seeded scaffolds were rinsed twice with PBS and then cultured in serum-deficient medium for 3 or 7 days. The metabolic activity of the cells seeded on the scaffolds was measured using the same colorimetric MTS assay described above ($n = 3$).

2.5. Effects of heparin on the growth of hSMCs

In order to determine whether heparin affects hSMC cell growth, we used two different approaches. First, we added heparin-containing medium to hSMCs that were seeded on tissue culture plates, and second, we added heparin-containing medium to hSMCs that had been seeded on electrospun PCL/gelatin scaffolds. For the first assay, hSMCs were seeded on 24-well tissue culture plates at a density of 1×10^4 cells/well and incubated in supplemented medium overnight. After rinsing the wells twice with PBS, serum-deficient media containing different concentrations of heparin (50 μg/ml and 100 μg/ml) were added to each plate. Cell growth at 3 and 7 days after heparin addition was assessed using an MTS assay, and these results were compared to those obtained from samples that were not treated with heparin (positive control). Similarly, for the second experiment, hSMCs were seeded at a density of 2×10^4 cells/scaffold in culture dishes, and these were incubated for 4–5 h to allow cellular attachment. The seeded scaffolds were then cultured overnight in supplemented medium. We used scaffolds that had not been conjugated with heparin for this experiment. The next morning, the scaffolds were rinsed twice with PBS, and the media was replaced with serum-deficient media containing heparin (50 μg/ml and 100 μg/ml). An MTS assay was performed at 3 and 7 days after addition of heparin, and this data was compared to data from cell-seeded scaffolds that had not been treated with heparin (positive control).

2.6. Cell proliferation and endogenous production of PDGF-BB

For the measurement of cell proliferation and endogenous PDGF-BB production, hSMCs (2×10^5 cells/scaffold) were seeded on the scaffolds created from various types of electrospun PCL/gelatin scaffolds: 1) unconjugated scaffolds (control), 2) heparin-conjugated scaffolds (HC), 3) PDGF/scaffolds (PDGF), and 4) PDGF/heparin-conjugated scaffolds (PDGF-HC). These cell-seeded scaffolds were cultured in SmBM medium as described above. To stimulate both cell proliferation and endogenous secretion of PDGF-BB by the cells, the medium was replaced every three days for culture periods of 1 and 2 weeks. At these predetermined time points, the medium was removed, and the cell-cultured scaffolds were washed, lyophilized, and stored at −80 °C. The samples were then digested in proteinase K solution [1 mg/ml proteinase K (Worthington, Lakewood, NJ, USA), 10 μg/ml pepstatin A, and 185 μg/ml iodoacetamide] at 56 °C for 16 h. Pepstatin A and iodoacetamide were used as proteinase inhibitors. Finally, aliquots from these digests were used to measure DNA content by a Picogreen dsDNA assay (Molecular Probes, Carlsbad, CA, USA) as well as to detect endogenous PDGF-BB by the human PDGF-BB ELISA Development Kit ($n = 3$).

2.7. Assessment of cellular infiltration

To evaluate the extent of cellular infiltration into the electrospun PCL/gelatin fibrous scaffolds, hSMCs (2×10^5 cells/scaffold) were seeded on scaffolds with three different fiber morphologies (1.0 μm fibers, co-electrospun fibers, and 3.0 μm fibers). Scaffolds with each of these fiber diameters were divided into the same groups as described above: 1) control, 2) HC, 3) PDGF, and 4) PDGF + HC. All of these cell-seeded scaffolds were cultured in the SmBM medium for up to 4 weeks, and the medium was changed every three days. At each time point, the retrieved cell-seeded scaffolds were fixed in 10% neutral buffered formalin and embedded in optimal cutting temperature (OCT) compound (Tissue-Tek®, Sakura Inc., Torrance, CA, USA). The samples were then cut into 10 μm thick sections to provide cross-sectional images of the scaffolds. The sectioned samples were fluorescently stained with 4'-6-diamidino-2-phenylindole (DAPI, Vector Laboratories, Burlingame, CA, USA) to visualize cell nuclei. In each group of samples ($n = 3$), both bright field and corresponding fluorescent images of the samples were acquired using a Leica DM4000 B microscope (Leica Microsystems, Wetzlar, Germany), and these images were merged together to define the boundaries of the cell-seeded scaffolds. The depth profiles of cellular infiltration were measured by overlaying a grid consisting of 50 μm thick lines onto the merged images. This allowed the number of cells to be counted and expressed as a percentage of the total cells in the images ($n = 3$). In addition, SEM was performed to observe the morphology of the cells on the surface of the cell-fiber constructs at each time point ($n = 3$). Formalin-fixed samples were washed with distilled water (three times), dehydrated through a series of graded ethanol solutions, and lyophilized overnight. Completely dried samples were sputter-coated with gold and observed using SEM.

2.8. Statistical analysis

All quantitative results are expressed as means ± standard deviation (SD) for n = number of samples analyzed. Statistical analysis was carried out using one-way ANOVA and Tukey's post-hoc analysis for multiple comparisons to determine significance. A value of either $P < 0.05$ or $P < 0.01$ was considered to be statistically significant depending on the experiment.

3. Results

3.1. Heparin-conjugated electrospun scaffolds and PDGF-BB immobilization

We fabricated electrospun PCL/gelatin scaffolds with three different fiber morphologies (Fig. 1B). By controlling the major electrospinning parameters (i.e. polymer concentration, electric field, and flow rate), PCL/gelatin scaffolds containing fibers of uniform diameter were produced. A 10% polymer solution produced fibers of 1.0 ± 0.1 μm in diameter, and a 15% polymer solution produced fibers of 3.0 ± 0.2 μm in diameter. In addition, we adopted a technique in which both the 10% and 15% solutions were co-electrospun. Co-electrospinning allowed us to obtain a construct in which fibers of both 1.0 and 3.0 μm existed, and these constructs could be consistently produced without any defects or size variations.

We fabricated heparin-conjugated scaffolds as well as bare fiber scaffolds for use as controls. Next, both heparin-conjugated and bare scaffolds were incubated with PDGF-BB; the heparin allowed electrostatic interaction of PDGF-BB with the scaffolds, while bare scaffolds passively adsorbed PDGF-BB. Morphological images of the scaffolds from both this passive adsorption of PDGF-BB and the specific interaction of PDGF-BB/heparin on the scaffolds, respectively, were compared to images of bare electrospun PCL/gelatin scaffolds (Fig. 1B). Although the processes of heparin conjugation and PDGF-BB immobilization were accomplished in the scaffolds, this appeared to result in a slight increase in fiber roughness regardless of fiber diameter when compared with the bare PCL/

gelatin scaffolds. However, despite the changes in fiber appearance in the heparin-conjugated scaffolds, these scaffolds retained their unique diameters and pore structures.

3.2. In vitro release kinetics of PDGF-BB from heparin-conjugated scaffolds

Fig. 2 shows the *in vitro* release kinetics of PDGF-BB from the electrospun PCL/gelatin scaffolds with or without heparin-conjugation. When PDGF-BB was loaded onto PCL/gelatin scaffolds that had not been conjugated with heparin (passive physical adsorption), an abrupt initial burst release occurred over the first 5 days of study. Specifically, over these first 5 days, the cumulative release of PDGF-BB from the unconjugated scaffolds was 7.7 ng/mg for the scaffolds with a fiber diameter of 1.0 μm, 4.8 ng/mg for the co-electrospun scaffolds with fiber diameters of 1.0 and 3.0 μm, and 3.9 ng/mg for the scaffolds with a fiber diameter of 3.0 μm. After this first 5-day period, only a very small additional release of PDGF-BB was seen over the next 15 days until the experiment was ended at 20 days. In contrast, when PDGF-BB was immobilized on the heparin-conjugated scaffolds, a sustained release of PDGF-BB was achieved, indicating that heparin conjugation could allow growth factors loaded onto a scaffold to be released in a controlled manner. When compared to the scaffolds that were not treated with heparin, those that were heparin-conjugated released only a very small amount of PDGF-BB over the course of 20 days, without the initial burst effect seen in the non-conjugated scaffolds. Over the 20 day time course, the cumulative amounts of PDGF-BB released from the heparin-conjugated scaffolds were 227 pg/mg for the 1.0 μm fiber diameter, 164 pg/mg for the co-spun scaffolds, and 91 pg/mg for the 3.0 μm fiber diameter.

3.3. Preservation of PDGF-BB bioactivity

The bioactivity of PDGF-BB that was both released from and bound to the electrospun scaffolds was determined by measuring the ability of PDGF-BB to stimulate hSMC proliferation. In Fig. 3, the scaffolds with different post-modifications stimulated a similar trend of cell proliferation in the cells cultured beneath them for 3 and 7 days using the Transwell® system. In addition, the cells proliferated in serum-deficient medium (1% FBS) over 3–7 days to a modest extent ($P < 0.05$). However, cells grown under the scaffolds which had undergone passive adsorption of PDGF-BB (PDGF) showed the highest proliferation at day 7, and this was statistically significant when compared to the others at day 7 ($P < 0.01$) as well as each corresponding sample at day 3 ($P < 0.01$). This remarkable increase in cell proliferation in the passively-adsorbed PDGF group was attributed to a rapid initial burst release of PDGF-BB at earlier time points, which was also shown in the in vitro PDGF-BB release profile (Fig. 2). However, a fiber diameter-dependent increase in cell growth as a function of culture time was not seen in this assay.

In Fig. 4, the bioactivity of the PDGF-BB that remained bound to the scaffolds was evaluated using a different approach. Here, cells were seeded and cultured directly on the various types of scaffolds for 3 and 7 days. Interestingly, cells cultured on the heparin-conjugated scaffolds which were immobilized with PDGF-BB (PDGF-HC) proliferated at the fastest rate when compared to the others ($P < 0.01$) and each corresponding sample at 3 days (co-electrospun and 3.0 μm fibers; $P < 0.05$). Unlike the data shown in Fig. 3, however, when cells were grown directly on the scaffolds, we were able to observe an effect of fiber morphology on cell proliferation. Cells tended to proliferate best on the scaffolds with the largest fiber diameter (3.0 μm), followed by the co-electrospun scaffolds and finally the 1.0 μm fibrous scaffolds. In fact, the cell growth in the 3.0 μm PDGF-HC group at 3 and 7 days was comparable or superior to the control group, which consisted of the same density of cells grown in a standard 24-well tissue culture plate. Cell proliferation in all the other groups was similar, but even here the tendency of fiber morphology to affect proliferation was evident. Thus, these data indicate that the biological activity of PDGF-BB bound to

heparin-conjugated scaffolds was preserved effectively, as its presence generated the best enhancement of cell proliferation.

3.4. Effects of heparin on the growth of hSMCs

Fig. 5 shows the effect of heparin on the growth profile of hSMCs. This experiment was performed by adding heparin-containing media (50 μg/ml or 100 μg/ml heparin in serum-deficient medium) to 24-well plates seeded with hSMCs (1×10^4 cells) as well as bare PCL/gelatin scaffolds seeded with hSMCs (2×10^4 cells). Inhibition of cell growth was calculated through comparison to appropriate positive control groups (samples of cells that were not treated with heparin-containing media) at day 3 and day 7. The results indicated that addition of heparin induced an approximately 30% inhibition of growth at day 3 of culture, and approximately 50% inhibition at day 7 compared with control groups at each time point (Fig. 5A, B). Growth inhibition was not dependent on heparin concentration. When heparin-induced growth inhibition was measured for cells growing on the bare PCL/gelatin scaffolds (Fig. 5C, D), we found that heparin almost completely inhibited growth of hSMCs on the PCL/gelatin scaffolds, and the cells arrested at a low level of metabolic activity.

3.5. Cell proliferation and endogenous production of PDGF-BB

Human SMC proliferation on the electrospun PCL/gelatin scaffolds was studied by measuring total DNA content. 2×10^5 cells were homogeneously seeded and cultured on the scaffolds for 1 and 2 weeks. As shown in Fig. 6, there was no significant difference in cell proliferation between the control, HC, and PDGF groups (Fig. 6A). However, it was apparent that the 3.0 μm fibers in the PDGF-HC group could stimulate cell proliferation remarkably well at both week 1 and 2, compared to the other groups ($P < 0.05$).

The endogenous production of PDGF-BB resulted in a similar pattern (Fig. 6B). All scaffolds in the PDGF-HC group encouraged a substantial increase in endogenous PDGF-BB production ($P < 0.05$, $P < 0.01$). In particular, the 3.0 μm and co-electrospun scaffolds in the PDGF-HC group induced greater secretion of PDGF-BB than the 1.0 μm fibers at 1 and 2 weeks. Therefore, it appears that not only exogenous PDGF-BB, but also endogenous PDGF-BB secreted by cultured hSMCs, contributes to the observed increase in cell proliferation on the 3.0 μm fibers in the PDGF-HC group.

3.6. Cell infiltration

Cellular infiltration into the electrospun PCL/gelatin scaffolds was investigated through histological staining and SEM analysis over a 4 week culture period (Fig. 7). All cells grown on 1.0 μm fibers were predominantly restricted to the surface of the scaffold. This phenomenon was seen in both histological and SEM analysis, both of which showed that the cells were spread out on top of the scaffold surface without any evidence of infiltration into the interior of the scaffold. Co-electrospun scaffolds could induce improved cellular infiltration compared to 1.0 μm fibers. This was ascribed to the increased size of the pore structure created by coelectrospinning of 1.0 μm and 3.0 μm fibers. The corresponding SEM images indicated that that the cells were likely to migrate just beneath the outer surface of the scaffold, but not deeper into interior sections. On the other hand, cells cultured on 3.0 μm fibers could penetrate the scaffold much better than those cultured on either 1.0 μm or co-electrospun fibers. These scaffolds were completely covered by proliferating cells and many had migrated beneath the surface. Most importantly, the PDGF-BB immobilized, 3.0 μm heparin-conjugated scaffolds demonstrated the most cellular infiltration of all the scaffolds. In the histological image, cells seeded and cultured on the top of these scaffolds had migrated almost all the way through the entire thickness of the scaffold mat. Taken together, these results suggest that the largest pores (porosity) generated by 3.0 μm fibers,

combined with the heparin-mediated delivery of PDGF-BB, could promote excellent cellular infiltration of a scaffold through a synergistic combination of physical (large pore) and chemical (PDGF-BB) cues. In Fig. 8B, the quantification of the cell infiltration data indicates that the PDGF-BB immobilized 3.0 μm heparin-conjugated scaffolds provided enhanced penetration over a depth range of over 200 μm ($P < 0.01$). However, there were no remarkable differences in between co-electrospun scaffolds and 1 μm scaffolds (Fig. 8A).

4. Discussion

Recently, a heparin-mediated delivery system for growth factors has been reported, and this system was shown to achieve the sustained release of heparin-binding growth factors while maintaining their bioactivity [19–23]. This system has been applied to a variety of tissue engineering scaffold materials, such as fibrin [24], collagen [21,22], chitosan-alginate [20], and poly(L-lactide-*co*-gly-colide) (PLGA) [23]. For example, Kuppevelt and colleagues chemically conjugated heparin to porous collagen scaffolds and showed that a homogenous distribution of growth factors such as bFGF and VEGF could then be achievedon these heparin-conjugated scaffolds [21]. Furthermore, binding of these growth factors to the heparin-ized collagen scaffolds was able to preserve their bioactivity, as this interaction with heparin appeared to protect the growth factors from denaturation and proteolytic degradation [19,25]. Consequently, when the heparinized collagen scaffolds with bFGF and VEGF were implanted subcutaneously, they could enhance angio-genesis significantly compared to non-heparinized collagen scaffolds with bFGF and VEGF [21,22]. It has also been shown that simple physical adsorption of growth factors onto scaffolds causes rapid diffusion from the scaffolds and decrease in their bioactivity, but heparin conjugation prevents this [26,27]. For instance, Shen et al. demonstrated that heparin-conjugated PLGA scaffolds provided a continuous bFGF release profile for over 2 weeks after a moderate initial burst release, which was mainly attributed to the strong electrostatic interaction between bFGF and heparin molecules [28]. On the contrary, they reported that most of the bFGF adsorbed onto bare PLGA scaffolds was likely to be desorbed into aqueous medium by a quick diffusion process.

In this study, we hypothesized that heparin-conjugated PCL/gelatin scaffolds fabricated by electrospinning could immobilize various growth factors, and that this property could be used to design a smart biomaterial system to enhance the functionality of tissue engineering scaffolds. In addition, we fabricated fibrous scaffolds with three different fiber morphologies to provide a series of fiber mats with graded surface area to volume ratios and porosities. The surface area to volume ratio increased (3.0 μm < co-electrospun < 1.0 μm) as the average fiber diameter decreased; on the other hand, the porosity increased as fiber diameter increased. We then selected PDGF-BB, which is a growth factor that possesses heparin-binding capacity [18], to use to test the release profiles and biocompatibility of these scaffolds. Here, in this *in vitro* release study, electrostatic interaction between cationic PDGF-BB (isoelectric point = 9.8) and anionic heparin molecules containing sulfonic groups ($-SO_3^-$) occurred, and this interaction controlled the diffusion of PDGF-BB in a steady and prolonged manner under the physiological conditions provided by the release medium. There are two distinct release mechanisms of growth factors from heparinized scaffolds: 1) an initial dissociation of surface-adsorbed growth factors to a moderate extent and 2) a sustained release of growth factors ruled by a thermodynamic equilibrium [28].

Based on the in vitro release kinetics of PDGF-BB (Fig. 2), it was noted that PDGF-BB was strongly bound to the heparin-conjugated PCL/gelatin scaffolds through electrostatic interaction. This could retard the dissociation of PDGF-BB from the scaffolds more effectively. Further, this means that much of the PDGF-BB that had been added to the scaffold remained bound to the fibers even after 20 days, suggesting that the scaffolds would

continue to slowly release the growth factor over an even longer time period. With respect to the effect of fiber morphology on PDGF-BB release, the data clearly show that the release of PDGF-BB from the scaffolds is fiber diameter-dependent, irrespective of heparin conjugation. This could be explained by the fact that the high surface to volume ratio created by the small fibers (1.0 μm in diameter) resulted in higher heparin conjugation efficiency, which was then followed by higher PDGF-BB loading efficiency. As a result, both the heparin-conjugated and unconjugated 1.0 μm fibrous scaffolds produced a higher cumulative release of PDGF-BB than the co-electrospun and 3.0 μm fibrous scaffolds. Although we did not determine differences in PDGF-BB loading efficiency between bare and heparin-conjugated PCL/gelatin scaffolds, there is much evidence in the literature suggesting that the chemical conjugation of heparin to scaffolds could significantly increase the loading efficiency of growth factors in a heparin/growth factor concentration-dependent manner [14,28]. In addition, it is generally accepted that the higher surface to volume ratio of electrospun scaffolds with smaller diameter fibers enables growth factors to be dissociated faster from the scaffold, since the release rate is directly related to the surface area that is exposed to the release medium [29].

Regarding the bioactivity of growth factors, it is generally known that the in vitro half-life of many growth factors is very short. For example, the half-life of bFGF has been found to be approximately 12 h [20]. This half-life is reduced even further once growth factors are intravenously administered for in vivo experiments. It is thus necessary to protect growth factors that will be used in vivo from thermal denaturation, enzymatic degradation, and inactivation at acidic pH. Such protection has been shown to occur through heparin binding, and results from a conformational change in the growth factor molecule during the binding process [30,31]. In this study, we showed that the in vitro bioactivity of PDGF-BB released from heparin-conjugated electrospun PCL/gelatin scaffolds is maintained. It has been demonstrated that bioactivity is preserved for an extended period when PDGF-BB is strongly bound to heparin-conjugated fibers. Thus, the high affinity of the heparin-conjugated scaffolds for growth factors can be essential in the design of novel scaffolds for tissue engineering applications, as the heparin molecules can serve to stabilize constructs loaded with growth factors and help to retain their biological activity and efficacy.

The anti-proliferative effect of heparin on vascular SMCs both in vitro and in vivo has been reported elsewhere for several decades [32,33]. Although the precise mechanisms governing this effect were not well known in detail, one possible mechanism may be that internalization of heparin into SMCs by receptor-mediated endocytosis activates intracellular pathways that suppress SMC growth [34]. In this study, the stability of the heparin-conjugated fibers had to be confirmed, and it was necessary to determine whether the potential release of heparin from these fibers could affect SMC proliferation in vitro. We have demonstrated that heparin is stable under similar conditions in which heparin-conjugated scaffolds were incubated for 10 days without any noticeable loss of bound heparin (data not shown). In summary, conjugation of heparin molecules to PCL/gelatin fibers could eliminate the inhibitory functions of free heparin on SMCs, because heparin is able to bind to these fibers in a strong and stable fashion.

The highest cell proliferation on the 3.0 μm fibrous scaffolds is likely due to the presence of exogenous PDGF-BB bound to the heparin-conjugated scaffolds as well as the relatively large pore structure formed by the 3.0 μm fibrous scaffolds. The influential impact of growth factor loaded and heparin-conjugated scaffolds has been demonstrated elsewhere to emphasize the role of incorporated exogenous growth factors with the sustained bioactivity [28]. Shen et al. reported that heparin-conjugated, bFGF-loaded porous PLGA scaffolds could induce significantly higher cell proliferation and viability when seeded with 3T3 fibroblasts than non-loaded scaffolds over a 10 day-period [28]. Moreover, Park et al.

designed a porous chondroitin-4-sulfate (CS)-chitosan sponge which was able to release PDGF-BB in a controlled manner [35]. As a result, a substantial increase in osteoblast proliferation was observed only in this PDGF-BB loaded CS-chitosan sponge compared to the CS-chitosan sponge without PDGF-BB incorporation. Akin to the endogenous secretion of PDGF-BB observed in Fig. 6B, it was previously investigated that a heparin-based hydrogel could tightly secure endogenous BMP-2 (secreted by cultured fibrochondrocytes) via high binding affinity to up-regulate the production of tissue-specific ECM components [36]. According to the literature, it has been well established that the exogenous addition of PDGF-BB would not only initiate DNA synthesis and mitosis of SMCs but also stimulate them to secrete endogenous PDGF-BB in an autocrine and paracrine manner [37].

Cellular infiltration or migration into electrospun nano-scaled fibrous scaffolds is often impeded due to the small pore size and high packing density of the fibers. Therefore, a variety of approaches have been undertaken to overcome this limitation. The effect of fiber diameter on cellular infiltration has been discussed extensively [38–40] and has also been demonstrated in the present study. Balguid et al. systematically evaluated the straightforward relationship between fiber diameter and cellular infiltration, which indicated that cell penetration could be encouraged proportionally with increasing fiber diameter [38]. Furthermore, it was found that larger fiber diameters might generate larger pore sizes in electro-spun fibrous scaffolds [2,39]. The inhibitory effect of nano-scaled fibers (below 1 μm in diameter) electrospun on top of existing micro-scaled fibers (above 3 μm in diameter) on cell infiltration was also investigated, and this study suggested that the denser nano-scaled fibers could prevent cells from migrating into the micro-scaled electrospun fiber structure [2,40].

5. Conclusions

We have demonstrated that the sustained release of PDGF-BB from an electrospun PCL/gelatin scaffold can be controlled by conjugating heparin molecules to the fibers. Moreover, a fiber diameter-dependent release pattern of PDGF-BB was observed during the course of the release test, and this effect occurred regardless of whether the fibers were heparin-conjugated. The biological activity of PDGF-BB (released from and bound to the electrospun scaffolds) facilitated cell proliferation significantly, which demonstrates that heparin conjugation provides prolonged preservation of the ability to stimulate hSMC growth. The secure binding of exogenous/endogenous PDGF-BB to the heparin-conjugated scaffolds would significantly improve the design and function of many types of tissue engineering applications in which the localized delivery of growth factors is desirable. Finally, the PDGF-BB loaded, heparin-conjugated 3.0 μm fibrous scaffolds promoted enhanced hSMC migration and infiltration into the scaffold. Therefore, we conclude that the combination of the large pore structures in the 3.0 μm fibers and the heparin-mediated delivery of PDGF-BB could induce the most effective cell infiltration into the scaffold via synergistic actions of physical and chemical cues.

Acknowledgments

The authors wish to thank Dr. Jennifer Olson for editorial assistance. This study was supported the Telemedicine and Advanced Technology Research Center (TATRC) at the U.S. Army Medical Research and Material Command (USAMRMC) through award W81XWH-07-1-0718 and the National Institute of Biomedical Imaging and Bioengineering (NIBIB) at the National Institutes of Health (NIH) through award 1R21 EB006539-01A2.

References

1. Sill TJ, von Recum HA. Electrospinning: applications in drug delivery and tissue engineering. Biomaterials. 2008; 29(13):1989–2006. [PubMed: 18281090]

2. Ju YM, Choi JS, Atala A, Yoo JJ, Lee SJ. Bilayered scaffold for engineering cellularized blood vessels. Biomaterials. 2010; 31(15):4313–4321. [PubMed: 20188414]

3. Lee SJ, Liu J, Oh SH, Soker S, Atala A, Yoo JJ. Development of a composite vascular scaffolding system that withstands physiological vascular conditions. Biomaterials. 2008; 29(19):2891–2898. [PubMed: 18400292]

4. Lee SJ, Yoo JJ, Lim GJ, Atala A, Stitzel J. In vitro evaluation of electrospun nanofiber scaffolds for vascular graft application. J Biomed Mater Res A. 2007; 83(4):999–1008. [PubMed: 17584890]

5. Burger C, Chu B. Functional nanofibrous scaffolds for bone reconstruction. Colloids Surf B Biointerfaces. 2007; 56(1–2):134–141. [PubMed: 17113762]

6. Szentivanyi A, Chakradeo T, Zernetsch H, Glasmacher B. Electrospun cellular microenvironments: understanding controlled release and scaffold structure. Adv Drug Deliv Rev. 2011; 63(4–5):209–220. [PubMed: 21145932]

7. Nie H, Ho ML, Wang CK, Wang CH, Fu YC. BMP-2 plasmid loaded PLGA/HAp composite scaffolds for treatment of bone defects in nude mice. Biomaterials. 2009; 30(5):892–901. [PubMed: 19010530]

8. Chakraborty S, Liao IC, Adler A, Leong KW. Electrohydrodynamics: a facile technique to fabricate drug delivery systems. Adv Drug Deliv Rev. 2009; 61(12):1043–1054. [PubMed: 19651167]

9. Yang Y, Li X, Qi M, Zhou S, Weng J. Release pattern and structural integrity of lysozyme encapsulated in core-sheath structured poly(dl-lactide) ultrafine fibers prepared by emulsion electrospinning. Eur J Pharm Biopharm. 2008; 69(1):106–116. [PubMed: 18078743]

10. Huang X, Brazel CS. On the importance and mechanisms of burst release in matrix-controlled drug delivery systems. J Control Release. 2001; 73(2–3):121–136. [PubMed: 11516493]

11. Lee J, Yoo JJ, Atala A, Lee SJ. Controlled heparin conjugation on electrospun poly(ε-caprolactone)/gelatin fibers for morphology-dependent protein delivery and enhanced cellular affinity. Acta Biomater. 2012; 8(7):2549–2558. [PubMed: 22465575]

12. Guan R, Sun XL, Hou S, Wu P, Chaikof EL. A glycopolymer chaperone for fibroblast growth factor-2. Bioconjug Chem. 2004; 15(1):145–151. [PubMed: 14733594]

13. Lyon M, Rushton G, Gallagher JT. The interaction of the transforming growth factor-betas with heparin/heparan sulfate is isoform-specific. J Biol Chem. 1997; 272(29):18000–18006. [PubMed: 9218427]

14. Sun B, Chen B, Zhao Y, Sun W, Chen K, Zhang J, et al. Crosslinking heparin to collagen scaffolds for the delivery of human platelet-derived growth factor. J Biomed Mater Res B Appl Biomater. 2009; 91(1):366–372. [PubMed: 19484776]

15. Nam J, Huang Y, Agarwal S, Lannutti J. Improved cellular infiltration in elec-trospun fiber via engineered porosity. Tissue Eng. 2007; 13(9):2249–2257. [PubMed: 17536926]

16. Baker BM, Gee AO, Metter RB, Nathan AS, Marklein RA, Burdick JA, et al. The potential to improve cell infiltration in composite fiber-aligned electrospun scaffolds by the selective removal of sacrificial fibers. Biomaterials. 2008; 29(15):2348–2358. [PubMed: 18313138]

17. W–lsh CJ, Schmeichel K, McBride K. Platelet-derived growth factor activates phospholipase D and chemotactic responses in vascular smooth muscle cells. Vitro Cell Dev Biol. 1991; 27A(5): 425–431.

18. Mangrulkar RS, Ono M, Ishikawa M, Takashima S, Klagsbrun M, Nowak RA. Isolation and characterization of heparin-binding growth factors in human leiomyomas and normal myometrium. Biol Reprod. 1995; 53(3):636–646. [PubMed: 7578688]

19. Gospodarowicz D, Cheng J. Heparin protects basic and acidic FGF from inac-tivation. J Cell Physiol. 1986; 128(3):475–484. [PubMed: 3528177]

20. Ho YC, Mi FL, Sung HW, Kuo PL. H-parin-functionalized chitosan-alginate scaffolds for controlled release of growth factor. Int J Pharm. 2009; 376(1–2):69–75. [PubMed: 19450670]

21. Nillesen ST, Geutjes PJ, Wismans R, Schalkwijk J, Daamen WF, van Kuppevelt TH. Increased angiogenesis and blood vessel maturation in acellular collagen-heparin scaffolds containing both FGF2 and VEGF. Bioma-terials. 2007; 28(6):1123–1131.

22. Pieper JS, Hafmans T, van Wachem PB, van Luyn MJ, Brouwer LA, Veerkamp JH, et al. Loading of collageneheparan sulfate matrices with bFGF promotes angiogenesis and tissue generation in rats. J Biomed Mater Res. 2002; 62(2):185–194. [PubMed: 12209938]

23. Yoon JJ, Chung HJ, Lee HJ, Park TG. Heparin-immobilized biodegradable scaffolds for local and sustained release of angiogenic growth factor. J Biomed Mater Res A. 2006; 79(4):934–942. [PubMed: 16941589]
24. Sakiyama-Elbert SE, Das R, Gelberman RH, Harwood F, Amiel D, Thomopoulos S. Controlled-release kinetics and biologic activity of platelet-derived growth factor-BB for use in flexor tendon repair. J Hand Surg Am. 2008; 33(9):1548–1557. [PubMed: 18984337]
25. Sommer A, Rifkin DB. Interaction of heparin with human basic fibro-blast growth factor: protection of the angiogenic protein from proteo-lytic degradation by a glycosaminoglycan. J Cell Physiol. 1989; 138(1):215–220. [PubMed: 2910884]
26. Bowen-Pope DF, Malpass TW, Foster DM, Ross R. Platelet-derived growth factor in vivo: levels, activity, and rate of clearance. Blood. 1984; 64(2):458–469. [PubMed: 6331547]
27. Yao C, Roderfeld M, Rath T, Roeb E, Bernhagen J, Steffens G. The impact of proteinase-induced matrix degradation on the release of VEGF from hepa-rinized collagen matrices. Biomaterials. 2006; 27(8):1608–1616. [PubMed: 16183114]
28. Shen H, Hu X, Yang F, Bei J, Wang S. Cell affinity for bFGF immobilized heparin-containing poly(lactide-co-glycolide) scaffolds. Biomaterials. 2011; 32(13):3404–3412. [PubMed: 21296407]
29. Okuda T, Tominaga K, Kidoaki S. Time-programmed dual release formulation by multilayered drug-loaded nanofiber meshes. J Control Release. 2010; 143(2):258–264. [PubMed: 20074599]
30. Prestrelski SJ, Fox GM, Arakawa T. Binding of heparin to basic fibroblast growth factor induces a conformational change. Arch Biochem Biophys. 1992; 293(2):314–319. [PubMed: 1536567]
31. Walker A, Turnbull JE, Gallagher JT. Specific heparan sulfate saccharides mediate the activity of basic fibroblast growth factor. J Biol Chem. 1994; 269(2):931–935. [PubMed: 8288646]
32. Clowes AW, Karnowsky MJ. Suppression by heparin of smooth muscle cell proliferation in injured arteries. Nature. 1977; 265(5595):625–626. [PubMed: 859561]
33. Hoover RL, Rosenberg R, Haering W, Karnovsky MJ. Inhibition of rat arterial smooth muscle cell proliferation by heparin. II. In vitro studies. Circ Res. 1980; 47(4):578–583. [PubMed: 6157501]
34. Castellot JJ Jr. Wong K, Herman B, Hoover RL, Albertini DF, Wright TC, et al. Binding and internalization of heparin by vascular smooth muscle cells. J Cell Physiol. 1985; 124(1):13–20. [PubMed: 3930515]
35. Park YJ, Lee YM, Lee JY, Seol YJ, Chung CP, Lee SJ. Controlled release of platelet-derived growth factor-BB from chondroitin sulfateechitosan sponge for guided bone regeneration. J Control Release. 2000; 67(2–3):385–394. [PubMed: 10825569]
36. Lee J, Choi WI, Tae G, Kim YH, Kang SS, Kim SE, et al. Enhanced regeneration of the ligament-bone interface using a poly(l-lactide-co-epsilon-caprolactone) scaffold with local delivery of cells/BMP-2 using a heparin-based hydrogel. Acta Biomater. 2011; 7(1):244–257. [PubMed: 20801240]
37. Sjolund M, Hedin U, Sejersen T, Heldin CH, Thyberg J. Arterial smooth muscle cells express platelet-derived growth factor (PDGF) A chain mRNA, secrete a PDGF-like mitogen, and bind exogenous PDGF in a phenotype- and growth state-dependent manner. J Cell Biol. 1988; 106(2): 403–413. [PubMed: 2828383]
38. Balguid A, Mol A, van Marion MH, Bank RA, Bouten CV, Baaijens FP. Tailoring fiber diameter in electrospun poly(epsilon-caprolactone) scaffolds for optimal cellular infiltration in cardiovascular tissue engineering. Tissue Eng Part A. 2009; 15(2):437–444. [PubMed: 18694294]
39. Eichhorn SJ, Sampson WW. Statistical geometry of pores and statistics of porous nanofibrous assemblies. J R Soc Interface. 2005; 2(4):309–318. [PubMed: 16849188]
40. Pham QP, Sharma U, Mikos AG. Electrospun poly(epsilon-caprolactone) microfiber and multilayer nanofiber/microfiber scaffolds: characterization of scaffolds and measurement of cellular infiltration. Biomacromolecules. 2006; 7(10):2796–2805. [PubMed: 17025355]

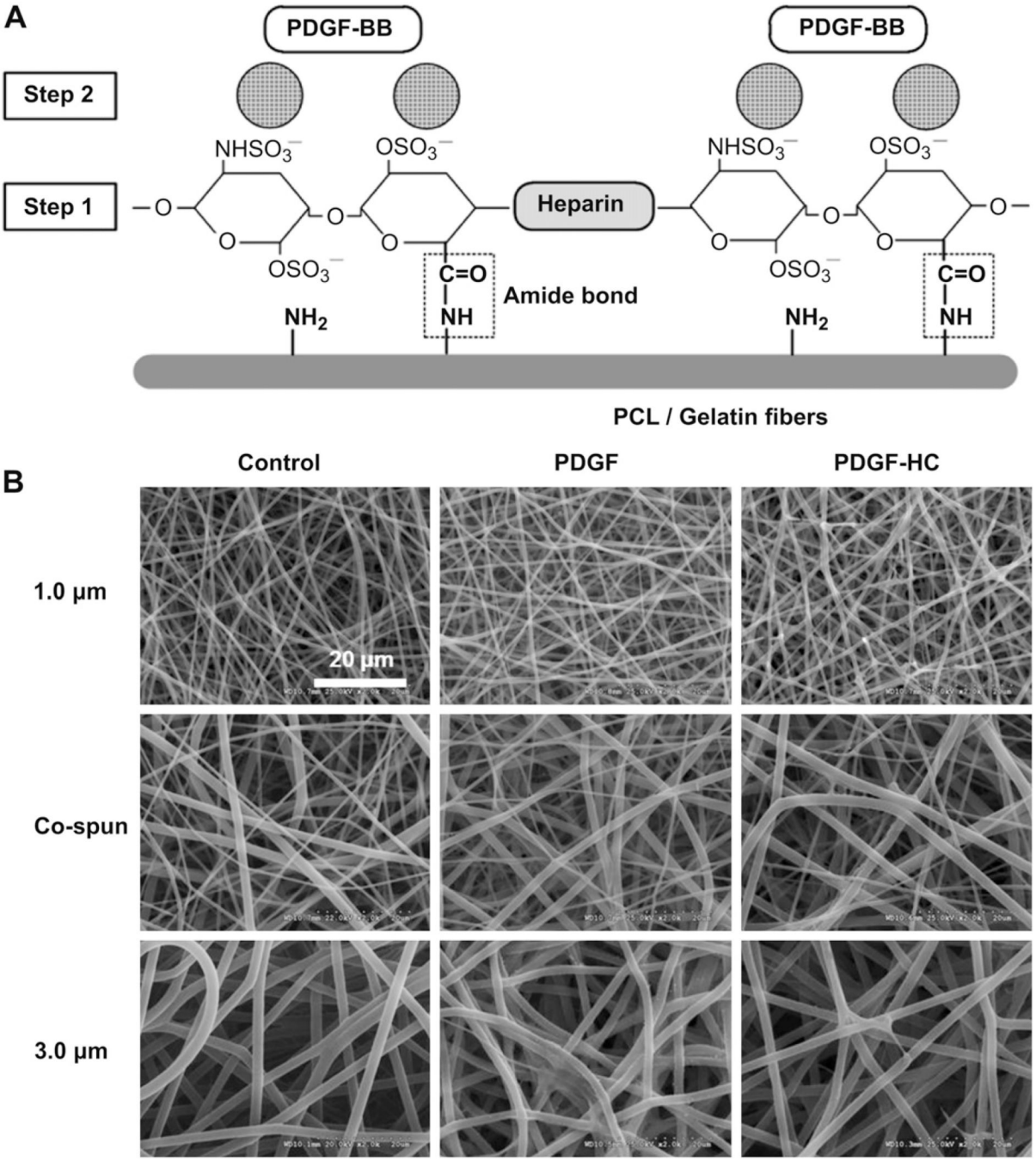

Fig. 1.

(A) Schematic diagram of PDGF-BB immobilization on heparin-conjugated electrospun PCL/gelatin fibers. [Step 1] heparin conjugation via the formation of amide bond. [Step 2] PDGF-BB immobilization through the electrostatic interaction between negative-charged heparin molecules and positive-charged PDGF-BB. (B) SEM images of (left column) electrospun PCL/gelatin fibers with three different fiber morphologies, (middle column) passive adsorption of PDGF-BB on the no heparin-conjugated fibers, and (right column) PDGF-BB immobilization on the heparin-conjugated fibers with a high affinity.

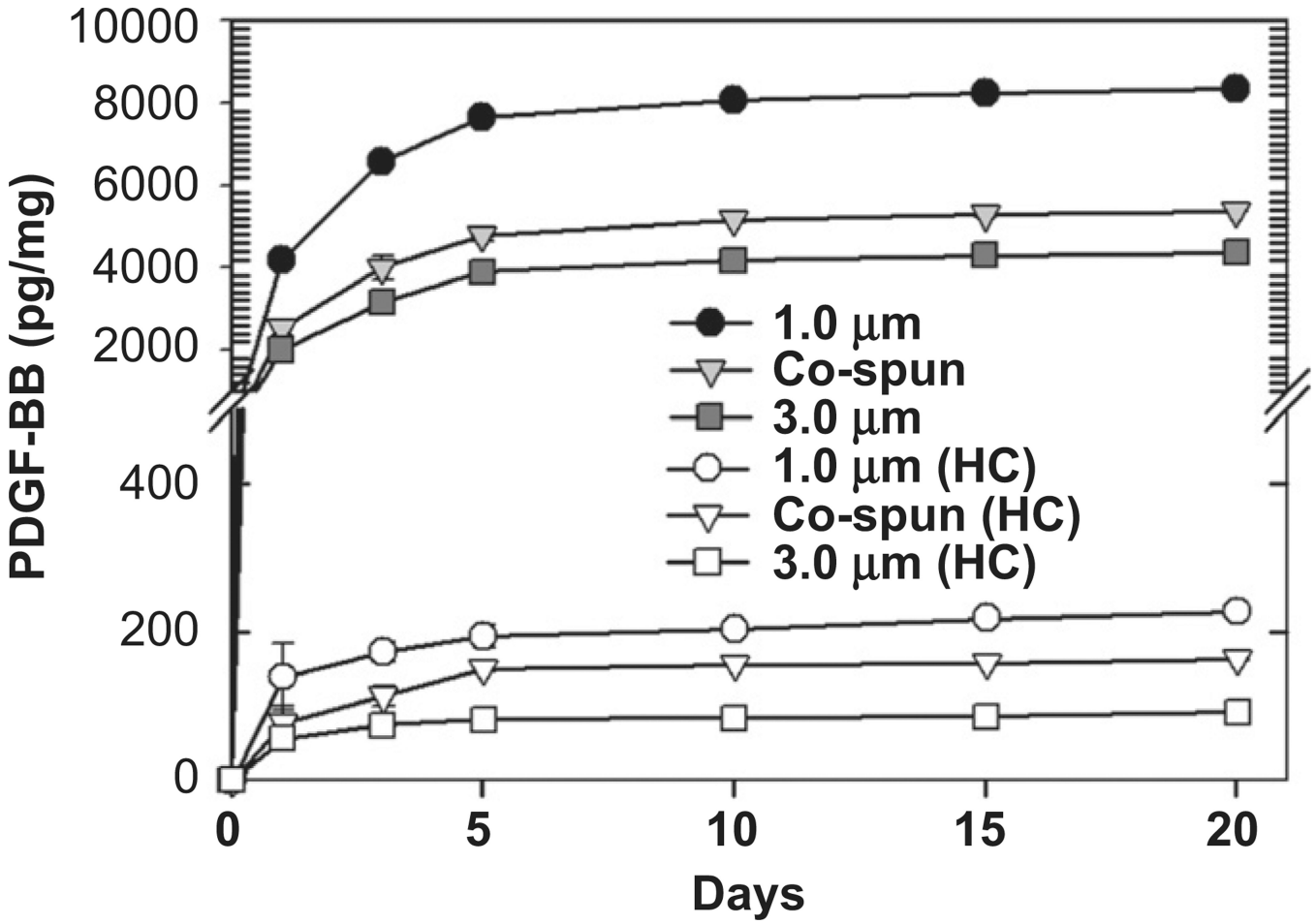

Fig. 2.
In vitro release kinetics of PDGF-BB from passively adsorbed on PCL/gelatin scaffolds (filled symbols) and heparin-conjugated scaffolds (open symbols).

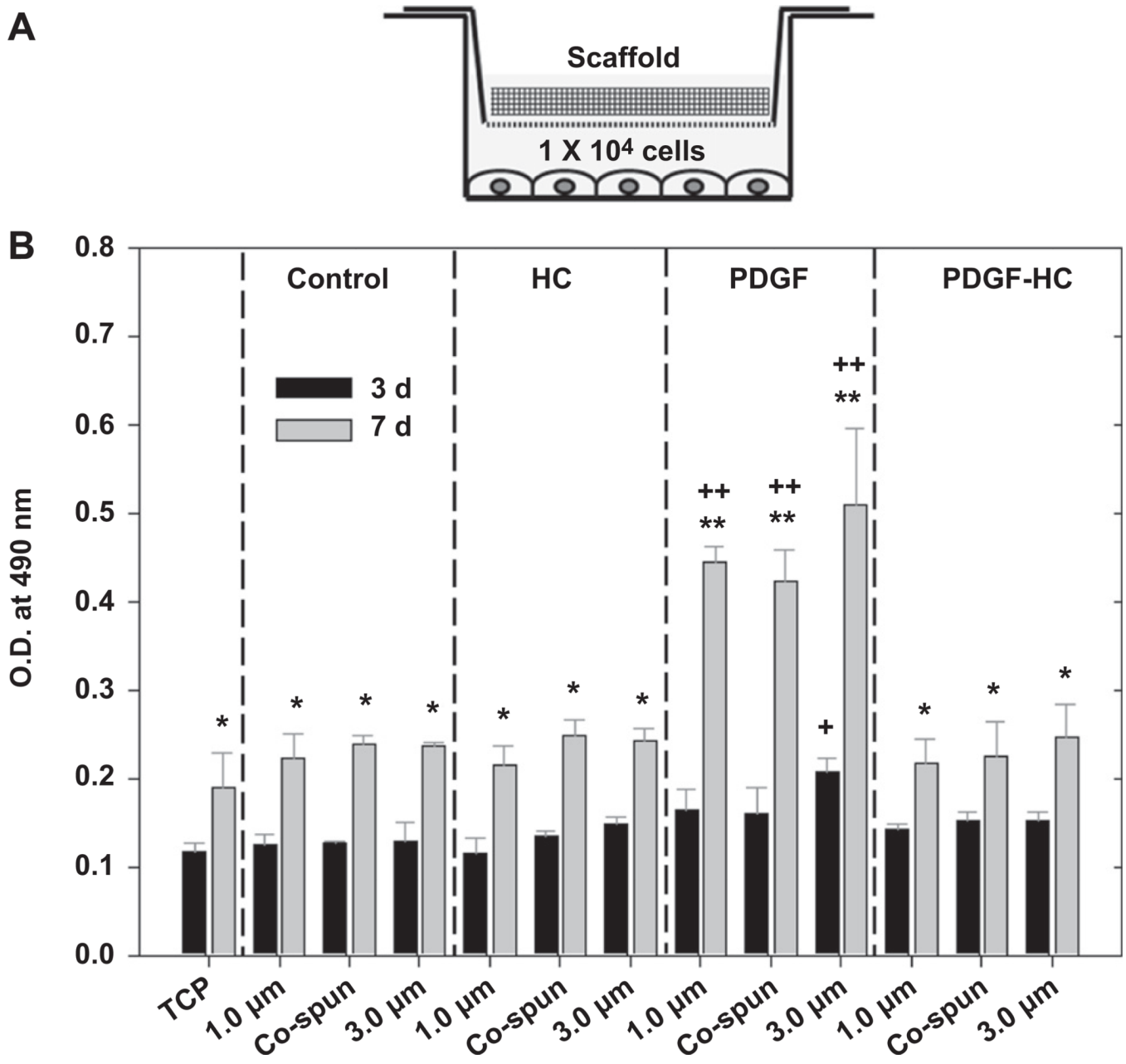

Fig. 3.

(A) Schematic illustration of experimental set-up for bioactivity test using Transwell® system. (B) Bioactivity of PDGF-BB released from the passively adsorbed scaffolds (PDGF) and the heparin-conjugated scaffolds (PDGF-HC). Tissue culture plates (TCP), unconjugated scaffolds (control) and the heparin-conjugated scaffolds (HC) without PDGF-BB were included for comparison. Statistical difference between day 3 and day 7 (*$P < 0.05$ and **$P < 0.01$) and comparison with control ($^{+}P < 0.05$ and $^{++}P < 0.01$).

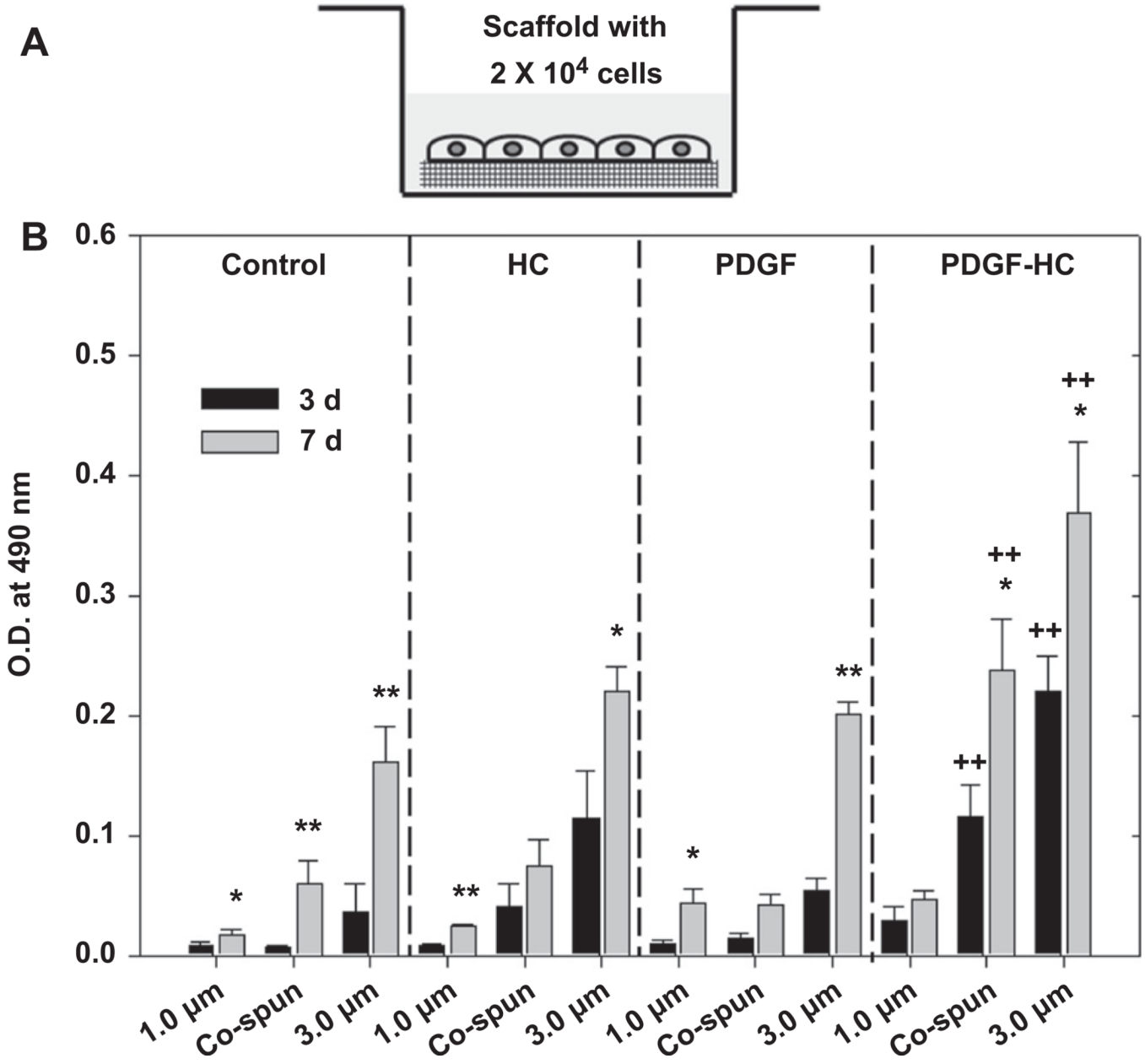

Fig. 4.

(A) Schematic illustration of experimental set-up for bioactivity test using Transwell® system. (B) Bioactivity of PDGF-BB released from the passively adsorbed scaffolds (PDGF) and the heparin-conjugated scaffolds (PDGF-HC). Tissue culture plates (TCP), unconjugated scaffolds (control) and the heparin-conjugated scaffolds (HC) without PDGF-BB were included for comparison. Statistical difference between day 3 and day 7 (*$P < 0.05$ and **$P < 0.01$) and comparison with control ($^{+}P < 0.05$ and $^{++}P < 0.01$).

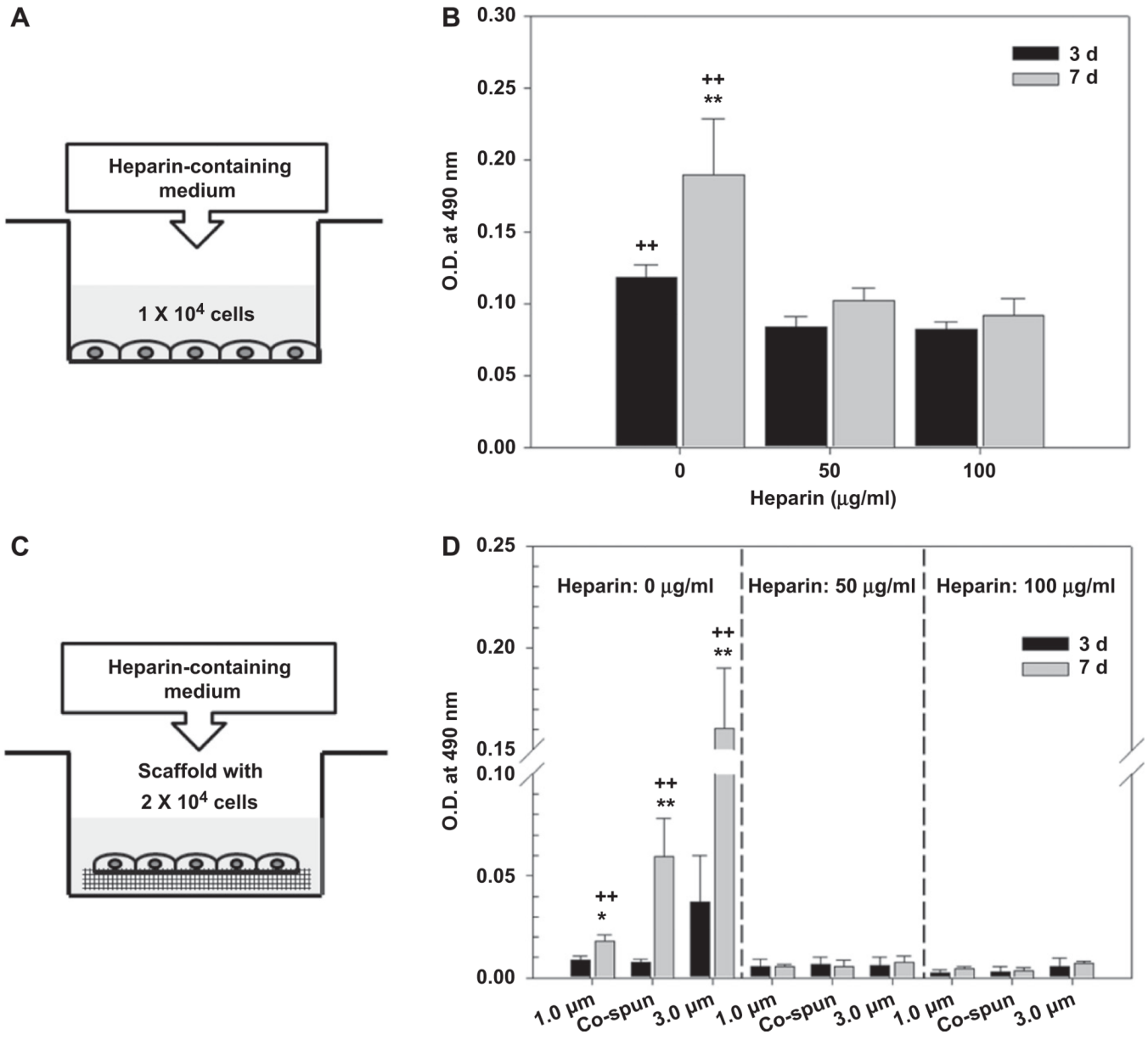

Fig. 5.

Anti-proliferative effect of heparin on hSMCs cultured on (A, B) 24-well tissue culture plates and (C, D) the bare electrospun PCL/gelatin scaffolds. Statistical difference between day 3 and day 7 (*$P < 0.05$ and **$P < 0.01$) and comparison with others ($^{+}P < 0.05$ and $^{++}P < 0.01$).

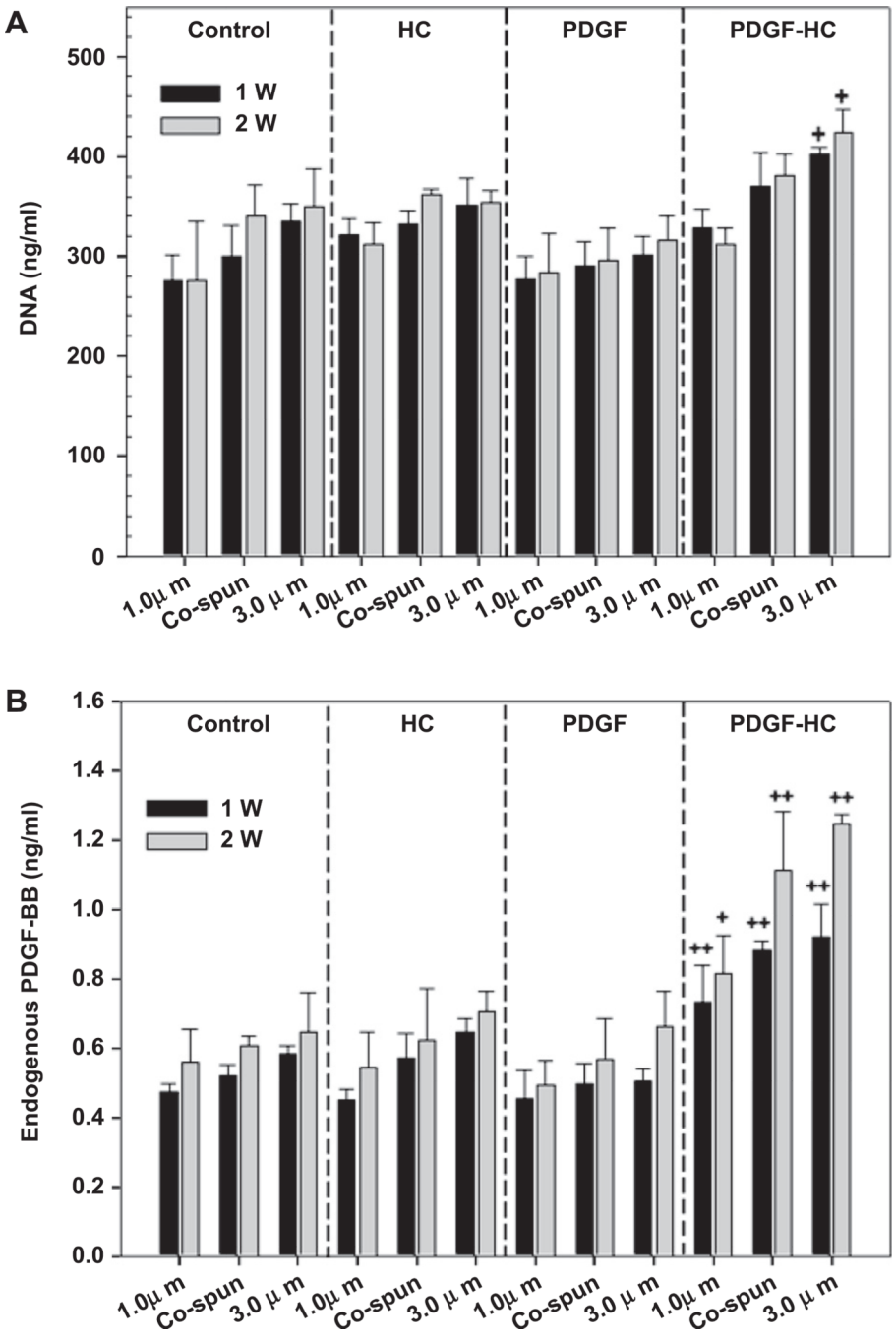

Fig. 6.

(A) Cell proliferation and (B) endogenous production of PDGF-BB secreted by the seeded hSMCs were assayed for the culture of 1 and 2 weeks, respectively (control, HC, PDGF, and PDGF-HC) ($^{+}P < 0.05$ and $^{++}P < 0.01$ compared to control).

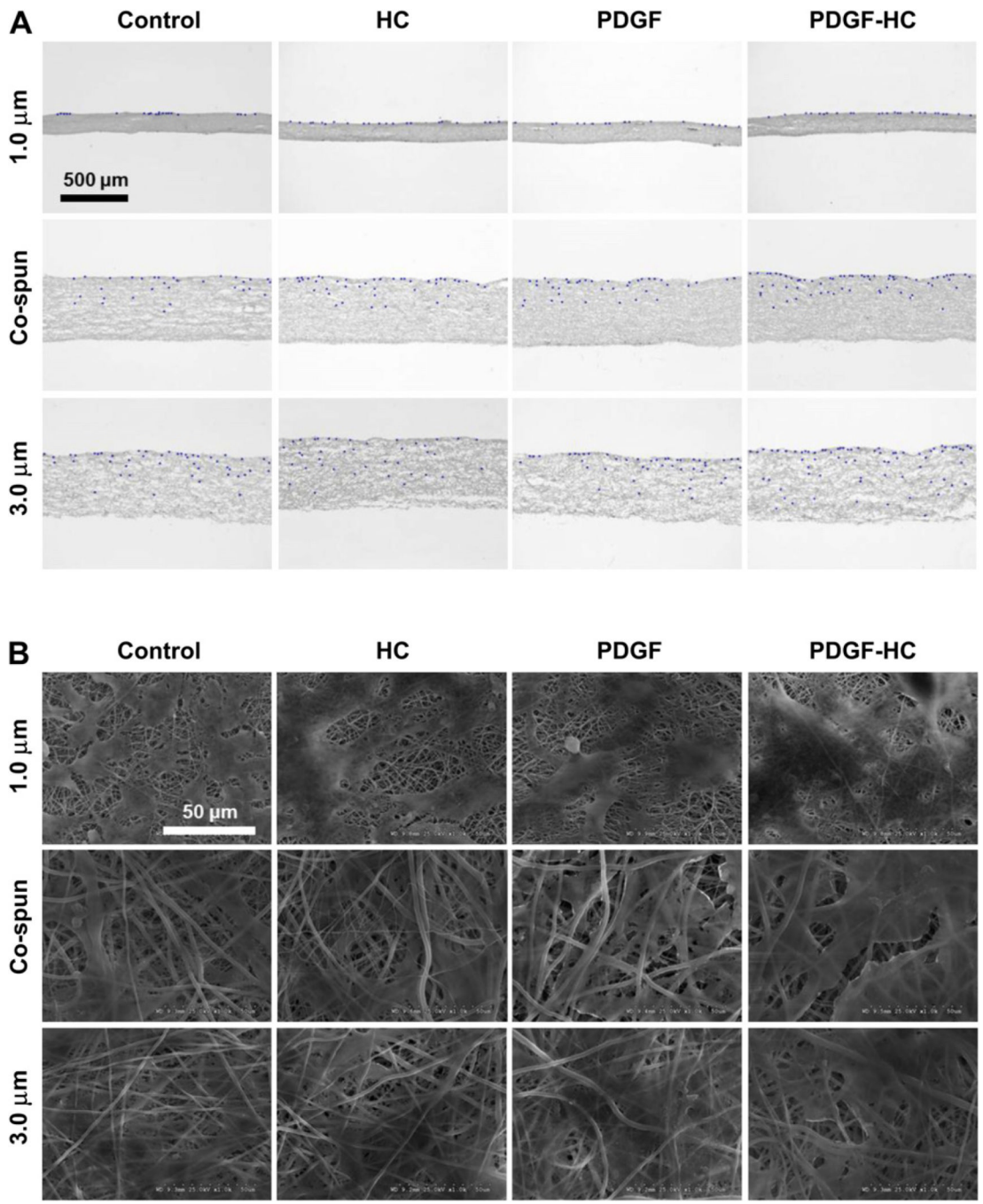

Fig. 7.

(A) Cellular infiltration into electrospun PCL/gelatin scaffolds after 4 weeks of hSMC culture (2×10^5 cells). Bright field and corresponding DAPI images were merged together using transverse-sectioned slides: control, HC, PDGF, and PDGF-HC (B) SEM images of hSMC seeded on the scaffolds at 4 weeks in culture.

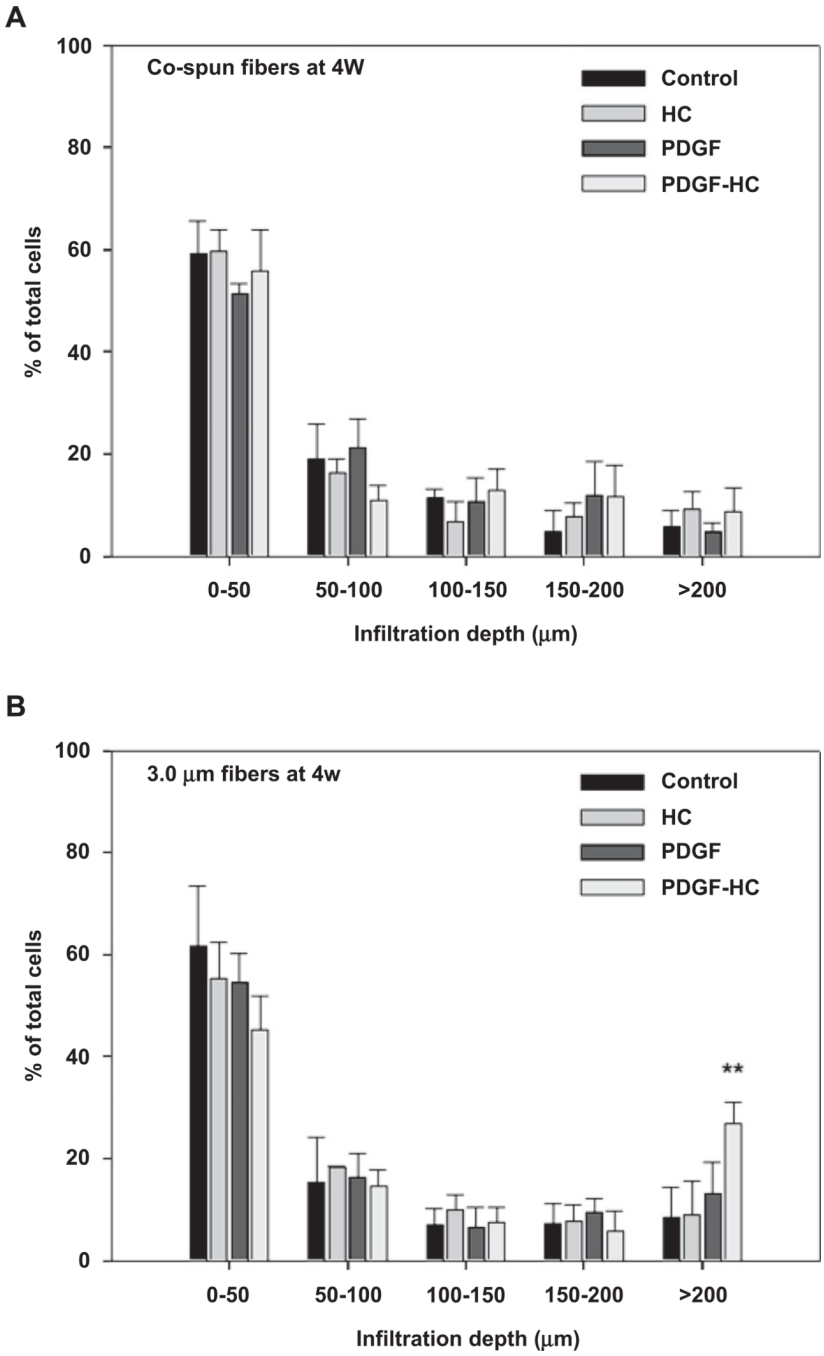

Fig. 8.

Quantitative analysis of SMC infiltration distance by proliferating cells on (A) co-electrospun and (B) 3.0 μm fiber scaffolds at 4 weeks of cell seeding: control, HC, PDGF, and PDGF-HC. For the analysis, a grid consisting of 50 μm thick lines was overlaid on the images shown in Fig. 7A and mean percentage of total cells at each depth range was then calculated (** $P < 0.01$ compared to others).